Optimisation of 3D printed concrete for artificial reefs: biofouling and mechanical analysis

Océane Ly [a], Adrian I Yoris-Nobile [b], Nassim Sebaibi [a,*], Elena Blanco-Fernandez [b], Mohamed Boutouil [a], Daniel Castro-Fresno [b], Alice E Hall [c], Roger JH Herbert [c], Walid Deboucha [a], Bianca Reis [d,e], João N Franco [d,e], Maria Teresa Borges [d,e], Isabel Sousa-Pinto [d,e], Pieter van der Linden [d,e], Rick Stafford [c]

[a] COMUE Normandie Université – Laboratoire Recherche Commun ESITC – ESITC Caen, 14610 Epron, France

[b] Universidad de Cantabria, 39005 Santander, Spain

[c] Bournemouth University, Poole, BH12 5BB, UK

[d] Faculdade de Ciências, Universidade do Porto, Rua do Campo Alegre s/n, 4150-181 Porto, Portugal

[e] CIIMAR, Centro Interdisciplinar de Investigação Marinha e Ambiental, Terminal de Cruzeiros do Porto de Leixões, Av. General Norton de Matos s/n, 4450-208 Matosinhos, Portugal

*Corresponding author: nassim.sebaibi@esitc-caen.fr

Abstract

Protection, restoration, and regeneration of aquatic habitats are an increasingly important issue and are requiring intensive research. In the marine environment, artificial reefs may be deployed to help offset habitat loss, increase local biodiversity and stimulate the recovery of ecosystems. This study aimed at the fabrication of artificial reefs by 3D printing. In the framework of the European INTERREG Atlantic Area collaborative project "3DPARE", six printed concrete formulations with limited environmental impact, based on geopolymer or cement CEM III binders and recycled sands, were immersed in the Atlantic along British, French, Portuguese and Spanish coasts. The colonisation of the concrete samples by micro- and macroorganisms and their durability were assessed after 1, 3 and 6 months of immersion. Results showed that both parameters were better with CEM III compared to geopolymer-based formulations. Therefore the use of CEM III should be prioritised over these geopolymer binders in 3D printed concrete for artificial reef applications.

Keywords: Artificial reef, 3D printing, Bio-receptive concrete, Geopolymer, Cement, Biofouling, Eco-engineering

1. Introduction

Artificial reefs are man-made structures deployed on the seafloor with a history that goes as far as back as the Roman Empire and Ancient Greece. Reefs were initially built for strategic military purposes such as the blockade of harbours or the trapping of enemy ships [1]. Yet artificial reefs now serve more specific objectives related to the restoration of fisheries and biodiversity and their deployment is often aimed at mitigating the effects of resource exploitation including destructive practices such as trawling [2]. Marine biodiversity provides beneficial ecosystem services such as commercial fisheries and tourism, including recreational scuba diving [3], so conservation and restoration is an imperative. Knowledge gained from the deployment of artificial reefs is also being applied to the ecological enhancement of other coastal structures [4].

Evidence of artificial reef works dating from 1789 has been found in Japan [5] and in the USA during the 19th century [6]. Their global deployment increased after World War II with the first national programmes in Japan [7] and later to other continents [8]. In Europe, many private or public-funded programmes were instigated in the Mediterranean Sea, however fewer have been deployed in the Atlantic area due to high storm frequency and strong currents in the benthic zone that make it much less stable and more difficult to study [9]. About 60 artificial reefs are listed in the OSPAR Maritime Area, from Norway to Portugal [10], 25 of which being in Spanish territorial waters [11]. Reefs in this area consist of car wrecks, shipwrecks, tyres and concrete blocks [12] [3] and geotextiles [13]. The design of concrete reefs has been very simple as they were made by casting fresh concrete into formwork and, in addition, the blocks were made of ordinary concrete [14]. Shapes varied from simple cubes or pipes called Bonna, to more elaborated geometric structures called Typi and Babel, deployed in chaotic or organised heaps, as seen on the French Atlantic coast [15]. First results of faunal monitoring studies on the Aquitaine coast in France showed the major presence of benthic fishes around the artificial reefs with higher taxa richness in more complex assemblies [16]. As complexity of design is important [12], but difficult to attain with conventional fabrication methods, 3D printing of concrete is a recent and promising technique which allows the design of very complex reefs (Fig. 1). In civil engineering, it consists of the upward fabrication of structures by the deposition of successive layers of concrete slurry with the help of a robotic arm or gantry. Debuts of 3D concrete printing for artificial reefs date from 2017 with projects in the Mediterranean Sea and in the Maldives.

Fig.1. 3D-printed artificial reefs submerged near Monaco coasts [17].

Artificial Reef 3D Printing for Atlantic Area (3DPARE) is a European project which gathers partners from France, Portugal, Spain and the UK. It aims to design and then fabricate 3D printed artificial reefs made of concrete to be deployed in the northern Atlantic area (Fig. 2). The first step was to optimise and choose the concrete formulations to facilitate colonisation and provide shelter to small and large species. The design aimed to be compatible with the marine environment, having less negative environmental impact, and to be chemically and physically resistant to marine conditions and stable on site against storms [18].

Fig.2. 3D-printed artificial reefs submerged

In the framework of 3DPARE project, these formulations are made from eco-friendly or recycled materials including crushed seashell sand, glass sand or geopolymer as a binder. Geopolymer binder is made of alumina-silicates, alkaline reagents such as sodium hydroxide NaOH or potassium hydroxide KOH, and water. They release less carbon dioxide in the atmosphere upon fabrication than ordinary Portland cement [19]. Other materials were also used, namely a ground granulated blast furnace slag cement CEM III which has been commonly used by the Dutch for a century in marine applications [20], and limestone sand.

While biofouling, *i.e.* the colonisation of wetted surfaces by biological microorganisms or macroorganisms, is more often overlooked in the case of marine infrastructures deployment i.e. Dikes, quay, etc – there is a large amount of literature on marine antifouling strategies. One major objective of this work is to get the highest rate possible of biocolonisation and biodiversity.

2. Experimental program

2.1. Materials used and sample preparation

To manufacture artificial reefs by 3D printing, six formulations made with geopolymer and cement mortars were analysed.

The terminology used for the identification of the formulations was the following: GL: geopolymer mortar with limestone sand; GG: geopolymer mortar with 30% glass sand; GS: geopolymer mortar with 50% shell sand; CL: cement mortar with limestone sand; CG: cement mortar with 50% glass sand; CS: cement mortar with 50% seashell sand.

The geopolymer mortars (GX) were manufactured with fly ash as the main binder; sodium hydroxide (NaOH), tap water, additives, and limestone sand, glass sand and seashell sand, as fine aggregates. On the other hand, cement mortars (CX) were manufactured with cement CEM. III/B 32.5 N-SR, tap water, superplasticiser as additive, fly ash and kaolin as additions; and the same fine aggregates used for the geopolymer mortars.

Fly ash was characterised by X-ray diffraction (XRD). For this, the ordinary range 10-80º (2θ) with the standard conditions for the diffractometer was explored working in the Bragg-Brentano configuration with a copper tube with filtration of the radiation K_β ($< \lambda >= 1.5418$ Å). The estimate of the amorphous contribution over the diffraction pattern was focused on $2\theta = 24.2°$, compatible with the amorphous phase of silicon oxide (SiO_2).

Fig. 3 shows the quantification of the possible crystalline phases, the most present being mullite ($Al_{4+2x}Si_{2-2x}O_{10-x}$): 44.4%; quartz ($\alpha$-$SiO^2$): 23.4%; maghemite ($\gamma$-$Fe_2O_3$): 21.2%; magnetite ($Fe_3O_4$): 8.4%; and corundum ($Al_2O_3$): 2.0%. Loss of weight by calcination (LWC) was 2.4%.

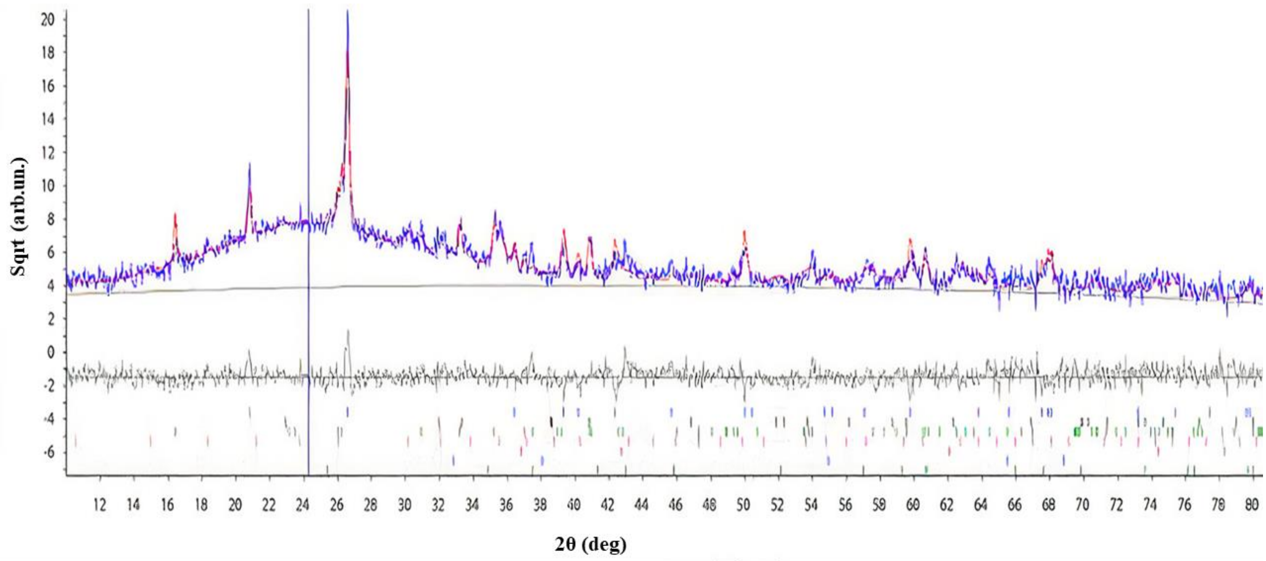

Fig. 3. Relative percentages over the total of crystalline phases (% in weight).

NaOH in industrial form with initial molar concentration 25 M was employed after dilution in tap water to be used as an activator. The solution was prepared at least one day ahead of use.

Cement type III/B had an ordinary content of 31% clinker and 66% steel slag (data provided by the manufacturer). The physical properties of cement used are summarized in Table 1. MetaKaolin was analysed by X-ray fluorescence spectrometry and its composition was shown in Table 2.

Table 1. Physical properties of cement

Blaine fineness (cm^2/g)	28 days compressive strength (MPa)	Setting time (min)	
		Initial setting time	Final setting time
4500	44	210	265

Table 2. Chemical composition of metakaolin (%)

SiO_2	Al_2O_3	Fe_2O_3	CaO	MgO	Na_2O	K_2O	TiO_2	LWC
48.3	35.5	1.5	0.24	0.4	0.1	1.35	0.28	12.5

Limestone sand, coming from quarry stone crushing, was provided in the fraction [0-3] mm. The crushed shells were obtained from the recycling of seashells coming from the canning industry. The glass came from smashed car windows in the fraction [0-0.3] mm. Fig. 4 represents the granulometric curves of the sands used in the mortars.

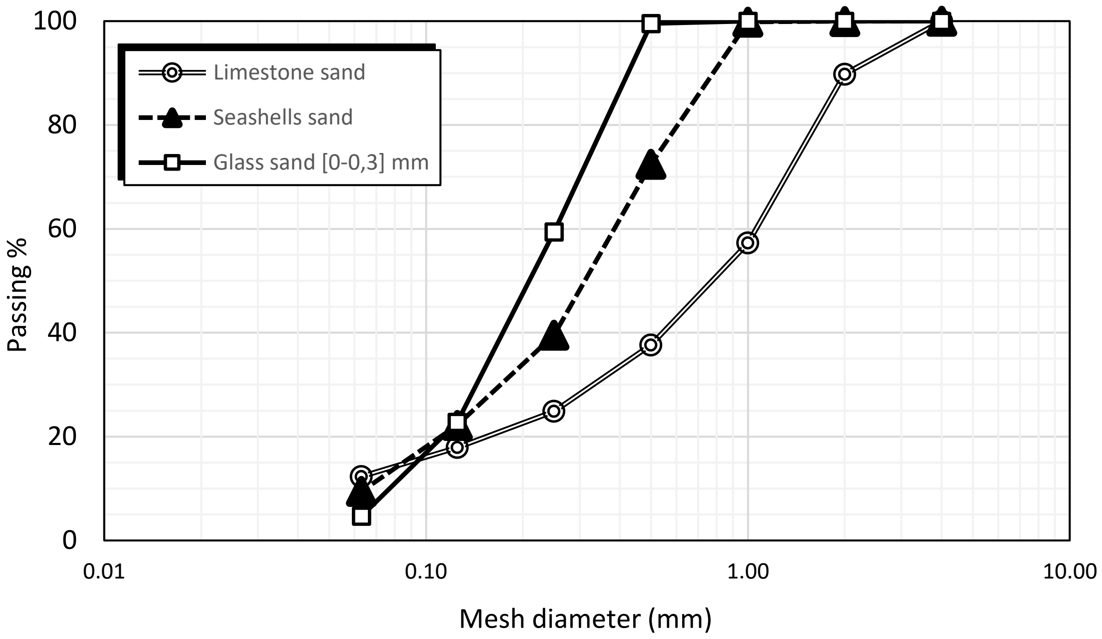

Fig. 4. Granulometric curves of the sands used in the mortars.

To carry out the experimental programme, 4 × 4 × 16 cm prismatic specimens were fabricated with a 3D printer type Delta of deposition per layer, whose maximal printing volume is 1 m diameter and 1 m height. The printer has a head which is composed of a hopper and a 3D worm drive inside, which, by spinning thanks to an electrical motor, drags the material to print towards the nozzle (Fig. 5a).

To obtain the prismatic specimens, mortar plates were printed with the 6 formulations under study, whose measurements were 40 × 51 × 6.4 cm. The plate perimeter was printed with a wall line, while the area was filled with lines at 45º (with respect to the perimeter) which alternated layer after layer (Fig. 5b). From each plate, 20 prismatic specimens were obtained, including two more than necessary in case any were damaged or there was any problem during sawing.

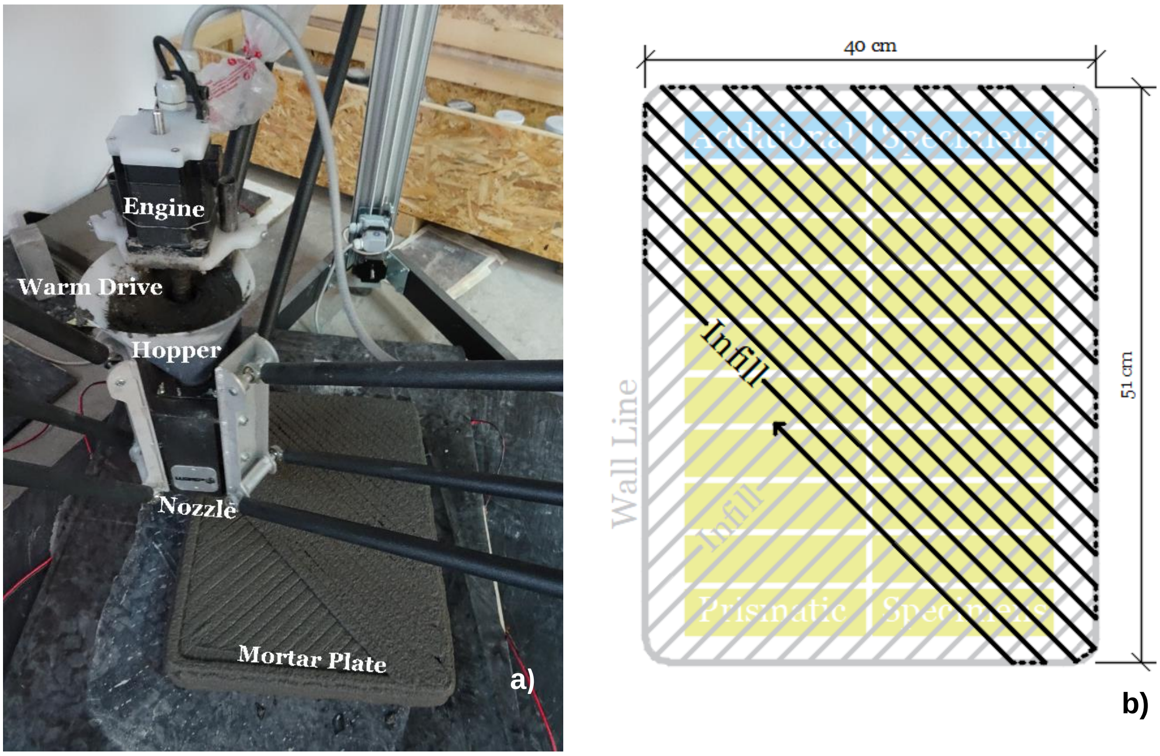

Fig. 5. a) 3D printer head details. b) Mortar plate printing and cutting scheme.

The distribution prismatic specimens was as follows: 4 partners (France, Spain, Portugal and United Kingdom); 6 different formulations; 5 immersion periods and one extra (1, 3, 6, 12, 24 months, extra); 3 replicates per formulation. This led to a total of 432 + 108 = 540 prismatic specimens.

The plates were printed with a nozzle of 20 mm diameter. A variable forward speed of the head of the printer was used, covering from 100 to 300 mm/s. The rotation speed of the worm drive to extrude the mortars was variable as well, going from 100 to 300 rpm.

From each plate, the required number of prismatic specimens by formulation was obtained for each partner. So, 6 mortar plates were fabricated per day, one plate for each formulation. In this way, the specimens corresponding to each partner were the same age.

After 7-14 days, the prismatic specimens were cut from plates with a circular saw. The cutting process was carried out carefully so as not to mix the different mortars nor losing the printing orientation. Once the cutting was completed, the upper printing face of the prismatic specimens were identified.

All mortars, both at the plate stage and also as prismatic specimens, were cured in air in a lab environment.

2.2. Protocol of 3D printed samples immersion

The specimens were printed in Spain and were consequently delivered to the other partners before they were 28 days. For the delivery, the specimens were fully wrapped in bubble wrap and laid in plastic boxes, to avoid damage. Upon arrival at destination, the bubble wrap was removed and the specimens were left in air in a lab environment. The immersion was carried out when the specimens were around 70 days.

At each location, the 18 specimens (3 replicates of 6 formulations) were fixed to plastic platforms and deployed in the sea. One platform was used for each age of immersion (in addition to an extra one set in case there was a problem). This paper indicates the results of the specimens with immersion periods of 1, 3 and 6 months, while those with periods of 12, 24 and extra are still immersed.

The platforms consisted of plastic boxes of 590 mm length, 365 mm width, 80 mm height and mesh opening 20 × 20 mm. The boxes were inverted sideways to lay the specimens. Initially, plastic separators with 1 × 1 cm of section were inserted between the box and the specimens; the specimens were placed according to the order and distances shown in Fig.6. Specimens were set between blocks (1 × 2 cm of section) to ensure that they could not move. Once the specimens were in place, they were fixed to the boxes with plastic cable-ties of 4 mm width. The fastening of the samples was done in a way that allowed the free circulation of seawater all around the samples.

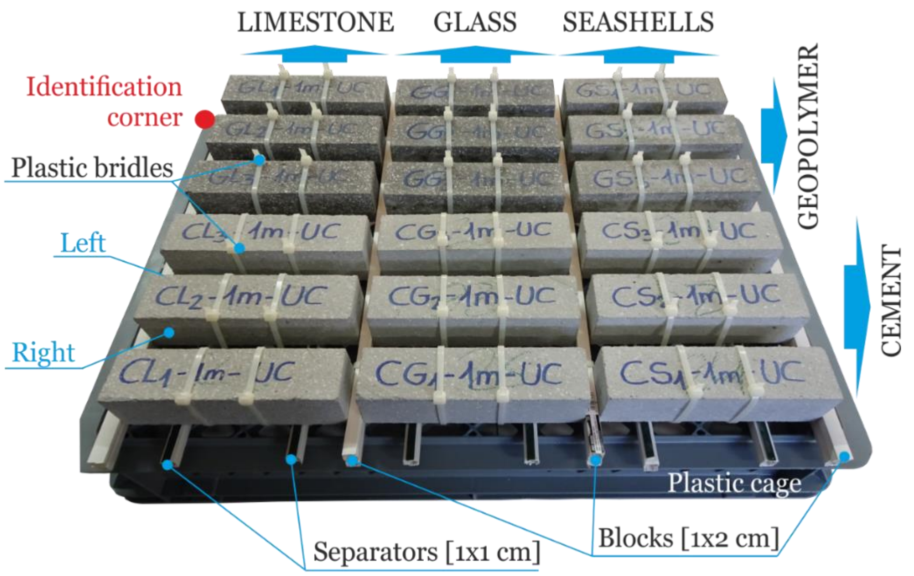

Fig. 6. Arrangement of specimens on the platform.

The platforms with the specimens were immersed in the sea, separated by at least 1 m from the seabed and 1 m from the sea surface. Platforms were deployed in relatively sheltered locations to ensure that they did not swing in waves . All samples were immersed in the North-east Atlantic Ocean, off the coast of England (Poole Bay), France (Saint-Malo Bay), Portugal (Matosinhos Bay) and Spain (Santander Bay). Cages were removed at 1, 3 and 6 months of submersion.

2.3. Monitoring protocol for the characterisation survey and post deployment of pilot reefs surveys

The main objective of artificial reefs is to enhance the biodiversity of the deployment site. For this, they first have to attract microorganisms which will colonise the material and become one of the first links in the food chain. Attractiveness of the samples to marine life was measured by two means: first, the visual assessment of the biocolonisation of the samples by image processing, and second, the amount of biomass of the micro- and macroorganisms attached to the samples. The first method gives clues about the surface area that is colonised by organisms, whereas the secondindicates the intensity of this colonisation. They thus provide complementary data on the bioreceptivity of the materials.

2.3.1. Visual assessment of biocolonisation by image processing

After the recovery of the samples at each time step, each of their sides (up, down, right, left) was immediately scanned on arrival at the laboratory on a Canon Lide 300 office scanner (Canon, Japan) with a 2400 × 4800 dpi resolution until the point at which they were colonised by macroorganisms. A scanner was preferred to photographs as it ensured the same image quality for all partners in terms of resolution, focal length or brightness. Scanned images were then processed on ImageJ (NIH, MD, USA) open source software.

The protocol for the scanned images processing was as follows: 1) definition of the region of interest (i.e. the samples boundaries) for each side; 2) 8-bit transformation of the raw image, assigning only grey values to each pixel, from 0 (black pixel) to 255 (white pixel); 3) thresholding: this allows to make the distinction between zones of interest (white colonised vs. black uncolonised); 4) computation of the percentage of covering: this value was defined considering the mean grey values (Eq. 1) of the samples following Eq. 2.

$$\text{mean grey value} = \text{sum of each side's grey values}/\text{number of pixels} \qquad (1)$$

$$\text{covering percentage } (\%) = (\text{mean grey value}/255) \times 100 \qquad (2)$$

2.3.2. *Biomass of collected micro- and macroorganisms*

When scanning was performed, the entire surface of the samples was scrubbed manually with a brush under distilled water in order to scrape off and collect all micro- and macroorganisms attached to the samples. The water containing the biomass was then filtered on 25-µm filter papers which were weighed after having being dried at 105 °C.

2.4. Mechanical tests

Mechanical tests were performed on the printed prismatic samples after the assessment of biocolonisation procedure. For this, flexural strength, compressive strength and Young's modulus were determined according to European standard EN 196-1, using an IGM 250 kN press (IGM, France), at 28 days of curing (reference properties), and at 1, 3 and 6 months after immersion. Briefly, a load of 0.05 kN/s was applied for the flexion test on the upper side of the whole prismatic sample according to the printing direction, until failure. The obtained halves of each sample then underwent the compression test on the same direction with a load of 2.4 kN/s. The Young's modulus was obtained measuring the slope of the compression curve between 30 and 80% of the compressive strength where the curve is the most linear.

3. Results and discussion

3.1. Biocolonisation

Biocolonisation and biomass results are summarised in Fig. 7 and 8, and Tables 3 to 5.

3.1.1. Image processing

Fig. 9 shows an example of raw scan image of one sample and the corresponding 8-bit and thresholded equivalent. It should be noted that no scanning was performed for 3 and 6 months samples from England and Portugal because of the presence of macroorganisms, as specified in the protocol mentioned in Paragraph 2.3.1 (Fig. 10). A general observation was that all samples were colonised as indicated by a noticeable change of colour (from grey and dark grey to brownish or greenish) However, biofouling was different according to the immersion location. In fact, colonisation was much higher in the southern part of the Atlantic (Portuguese and Spanish northern coasts) compared to its northern part (British and French coasts). Results may appear mitigated, for samples – especially the French ones – for which the colonisation was visually difficult to assess. For these, results were highly dependent on the eye and discrimination capacity of the experimenter; however this bias was reduced by ensuring that all image analyses were carried out by the same person. On the contrary, highly colonised samples – like Portuguese and Spanish ones – were unequivocal.

UK 1 month results (Fig. 7a) showed that the best colonisation rates were observed for CG and CL with a covering percentage of 44.6% and 43.8% respectively. CL is closely followed by GL with 43.1% of the surface covered. A quite different rank was found for Portuguese 1 month samples (Fig. 7b), dominated by CS (92.1%) followed by GS (87.4%) and CG (87.3%) on the last step. Here again, the second and third best results are similar. With the French and the Spanish results at 1 month of immersion (Fig. 8), it appears that generally, the best colonisation behaviour is observed for CX samples whereas it is less good with GX samples, though this is less true for Spanish 3 months results. The hypothesis is that geopolymers leach high amounts of OH^- which affect the pH of the local habitat (between 7.4 and 7.6 for seawater according to [21] and [22]), making it more alkaline. This release can lead for some cases to a soaring pH of deionised water in a logarithmic trend from up to more than 10 in tens of minutes at 90 °C [23]. Yet a modification of pH to extremes – either basic or acid – is known to be adverse to marine organisms. Indeed, pH can be used by potential basibionts (*i. e.* living organisms as substrates) in their immediate vicinity as a chemical deterrent against epibionts (*i. e.* organisms living on the surface of another living organism) in an antifouling defence strategy [24]. However, [25] showed that the pH decreases slowly, from 11.3 to 10.2 on average up in 60 mL of distilled water over 28 days. We can assume that the decrease of pH is more important in the large quantity of water represented by the sea, and that dilution compensated the early "toxicity" of geopolymer towards microorganisms later on. Portland blast furnace slag cement also leads to an increase of pH but the variation appears much less important than with geopolymers, about 0.2 after 7 days in artificial seawater [26].

Despite those differences, we can see with the French and Spanish samples (Fig. 8) that all samples follow the same trend, namely the tendency of the biofilm to cover the whole surface of the samples, and we can assume that this is the same for the British and the Portuguese samples. In some way, it supports the notion that all materials will be colonised to some extent, even if it were toxic on its surface or by leaching, as claimed in the literature [27] [28]. Nevertheless, as they were tied to platforms with cable ties which hide a small part of the available surface to colonisation accounting for uncolonised zones, biofouling will never reach 100%.

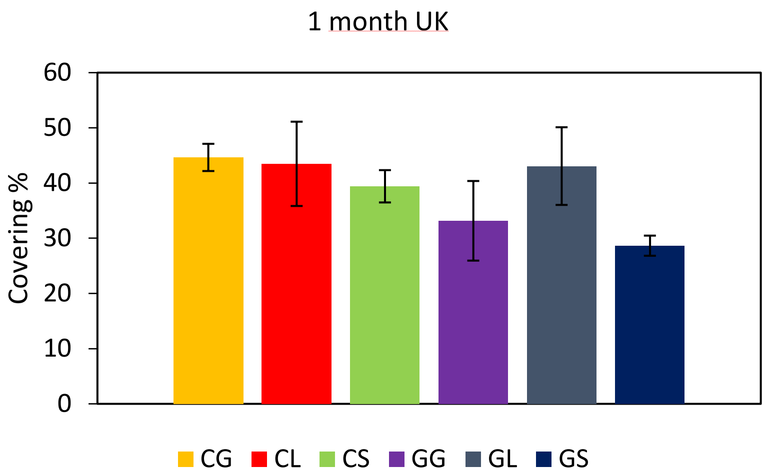

a)

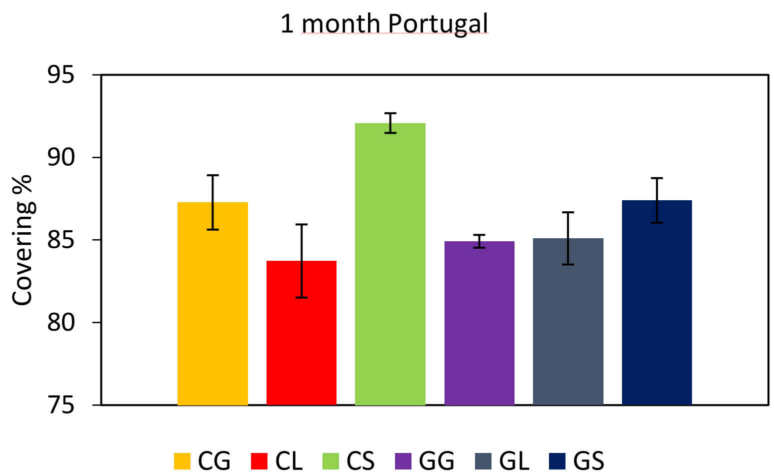

b)

Fig. 7. Mean biocolonisation coverage per material tested at 1 month, obtained from scanned images for a) the UK, b) Portugal.

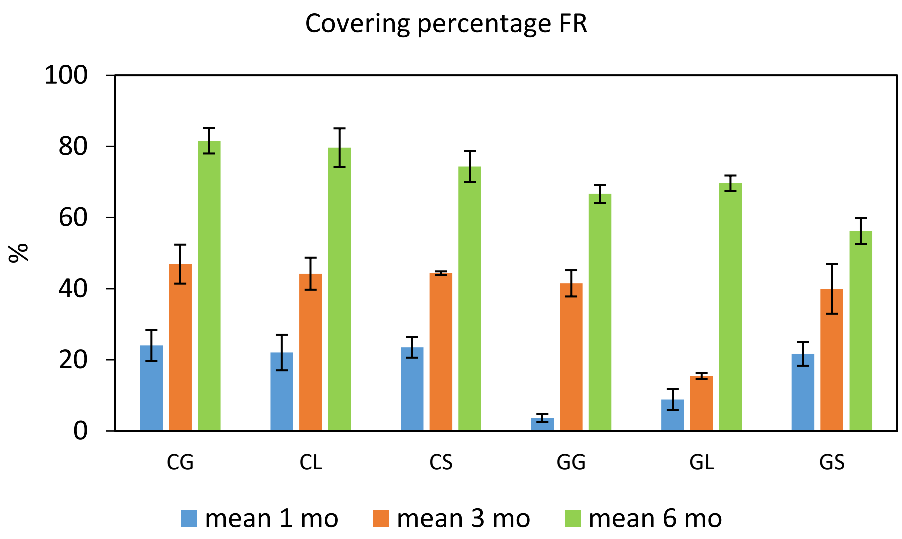

a)

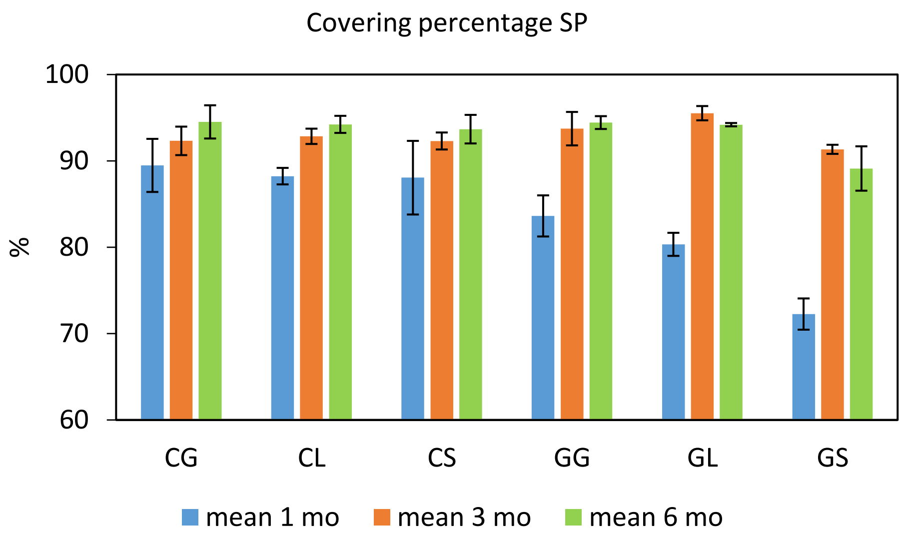

b)

Fig. 8. Mean biocolonisation coverage per material tested at 1, 3 and 6 months, obtained from scanned images for a) France, b) Spain.

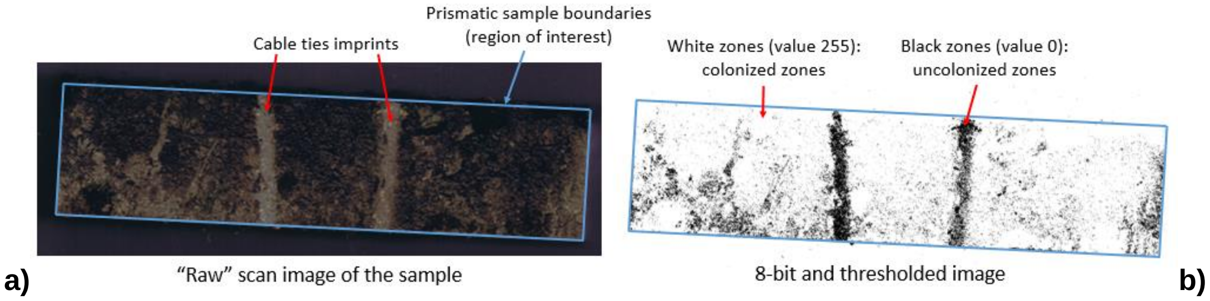

Fig. 9. Image processing: a) "Before" unprocessed scan image; b) "After" 8-bit and thresholded black and white image.

Fig. 10. Example of sample partially covered with macroorganisms (mussels, ascidians). Samples with macroorganisms attached were not scanned, only biomass was measured.

3.1.2. Biomass

Slightly higher values are observed on average with GX bricks compared to CX for 1 and 3 months (means of 1.74 g vs. 1.87 g and 8.1 g vs. 9.65 g respectively, Tables 3 and 4), but the association is reversed at 6 months of immersion (mean of 8.03 g for CX vs. 6.03 g for GX, Table 5). These differences vary from 0.13 g at 1 month to 2 g at 6 months. These values contrast with visual biocolonisation results for which CX were generally superior ; it might indicate that the biofouling is more important and more localised for GX samples, while for CX samples the layer of biofouling is thinner but larger in surface area. Finally, we noted that, as for coverage, the collected biomass increased over time for all samples. This is due to the extended spreading of biofouling on the surface but also to the increase in thickness of the biological layer. This observation confirms the fact that once the first microorganisms are established, they can develop to their maximum stage of maturation. It is therefore promising for the attraction of macro species and the enhancement of the local habitat with more species and more individuals. Regional variation in biofouling coverage and biomass could be due to multiple abiotic factors, notably seawater temperature, turbidity and levels of nutrients including nitrates and phosphates. There is also the possibility of biological interactions such as the abundance of local grazers and predators.

Table 3. First month biomass dry weight data for materials tested in France (FR), the UK, Spain (SP) and Portugal (PT) and overall average.

1 month	FR [g]	UK [g]	SP [g]	PT [g]	**AVERAGE [g]**
CL	1.07	0.49	2.65	1.11	**1.33**
CS	0.67	0.34	2.57	1.07	**1.16**
CG	0.03	0.57	9.19	1.09	**2.72**
GL	0.02	0.72	5.06	1.24	**1.76**
GS	0.04	0.37	2.31	1.61	**1.08**
GG	0.79	0.37	8.48	1.41	**2.76**

Table 4. Three months biomass dry weight data for materials tested in France (FR), the UK, Spain (SP) and Portugal (PT) and overall average.

3 months	FR [g]	UK [g]	SP [g]	PT [g]	**AVERAGE [g]**
CL	0.65	7.06	19.06	8.38	**8.79**
CS	0.63	5.95	14.09	10.28	**7.74**
CG	0.74	4.41	16.07	9.87	**7.77**
GL	0.99	4.62	22.63	9.77	**9.50**
GS	1.37	5.96	23.13	6.55	**9.25**
GG	1.08	5.86	19.32	14.53	**10.20**

Table 5. Six months biomass dry weight data for materials tested in for France (FR), the UK, Spain (SP) and Portugal (PT) and overall average.

6 months	FR [g]	UK [g]	SP [g]	PT [g]	**AVERAGE [g]**
CL	1.78	5.91	8.20	17.89	**8.44**
CS	2.14	7.16	7.88	17.84	**8.75**
CG	1.91	5.94	9.93	9.80	**6.89**
GL	1.12	4.16	8.09	11.38	**6.19**
GS	1.90	4.23	8.85	9.73	**6.18**
GG	1.86	4.36	6.91	9.74	**5.72**

3.2. Mechanical results

Reference mechanical tests results obtained at 28 days of curing are presented in Fig. 11.

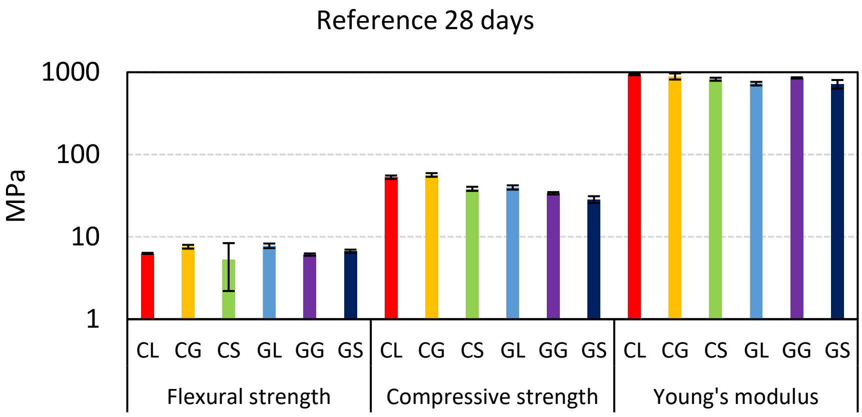

Fig. 11. Reference mechanical properties for tested materials at 28 days.

Mechanical tests results show the same trend over time, across all regions. Although different values were obtained from each region, the trend is similar for all three studied mechanical properties (flexural strength, compressive strength, Young's modulus). An example of what was observed for all regions is shown in Fig. 12. For each region and at each due time, even at 28 days,we observed better mechanical behaviour with CX samples than with GX except for GL which is comparable to CS.

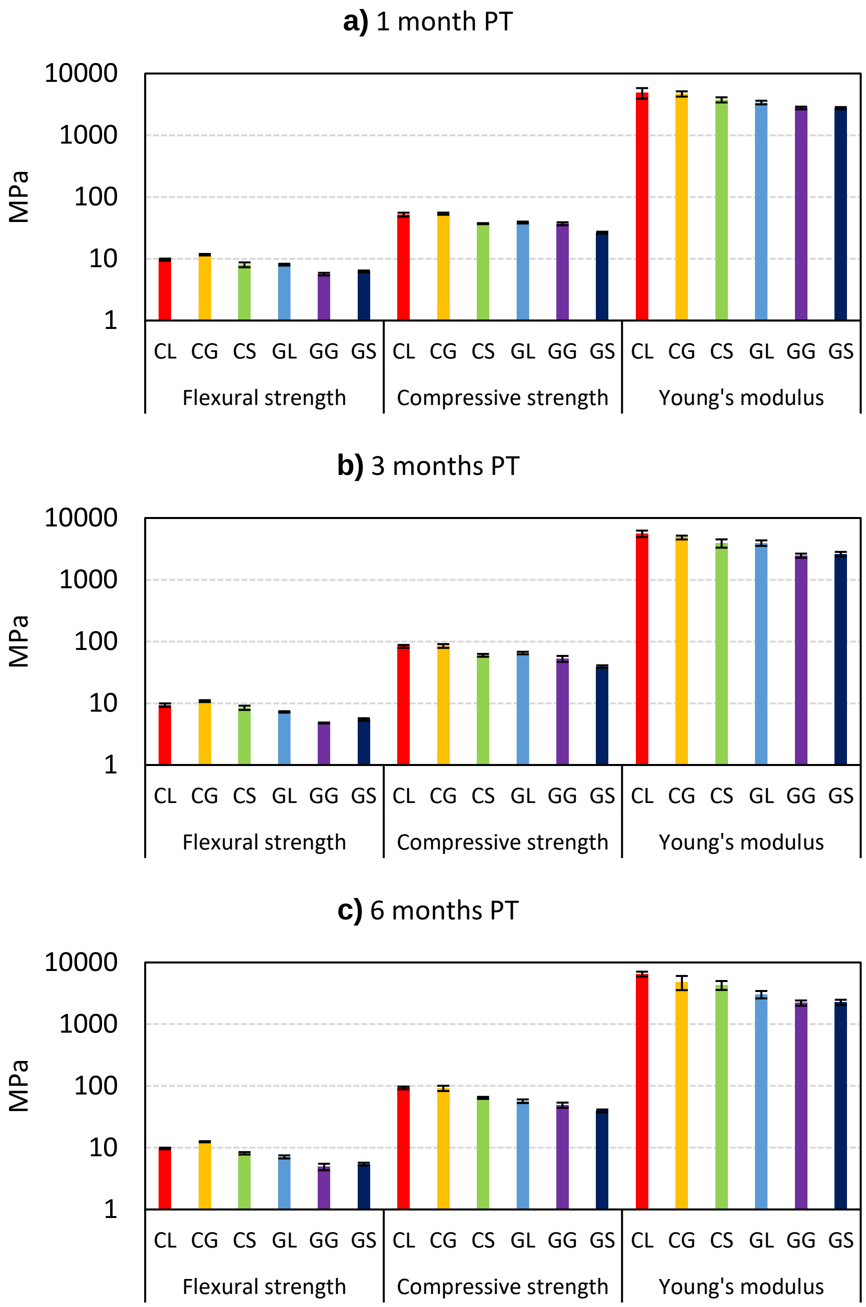

Fig. 12. Example of mechanical properties over time obtained for Portuguese samples at a) 1 month, b) 3 months, c) 6 months of submersion.

While averaging the mechanical properties values from all regions (Fig. 13), this association is even more clear , especially for the compressive strength and the Young's modulus with differences up to 50 MPa and 2 GPa respectively (CG vs. GS at 6 months). The flexural strengths are more alike and do not vary much over time compared to the other two mechanical properties. A major observation is the increase in compressive strength for both CX and GX, with a higher variation for CX. These results are consistent with the literature, as long term studies show that geopolymers can achieve 70% of their one-year compressive strength at 3 days, indicating a still-going geopolymerisation process [29]. This increase is slow [30] compared to CEM III the slow hydration process of which continues on the long term and highly contributes to the enhancement of ground granulated blast furnace slag cement performance. In fact, CEM III can achieve 128% of its 28-day strength at 180 days [31].

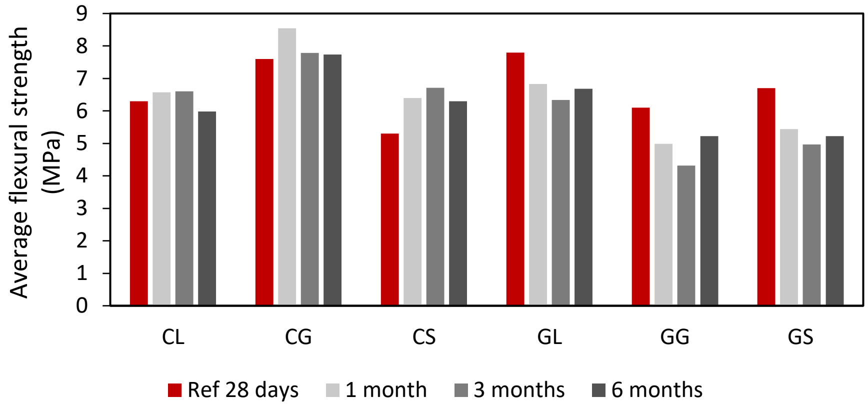

a)

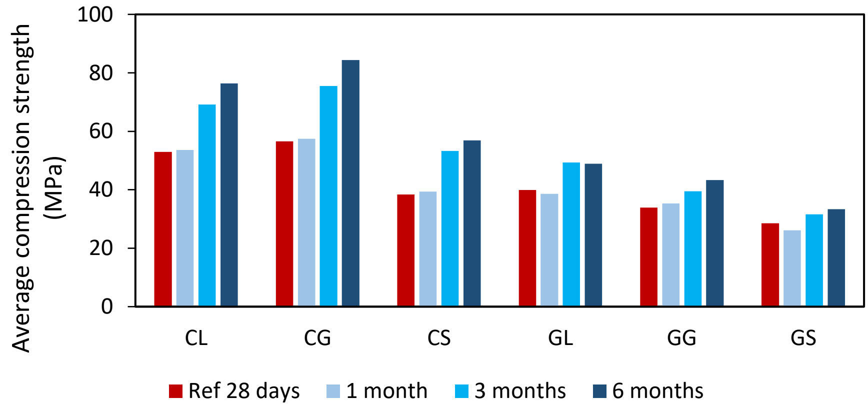

b)

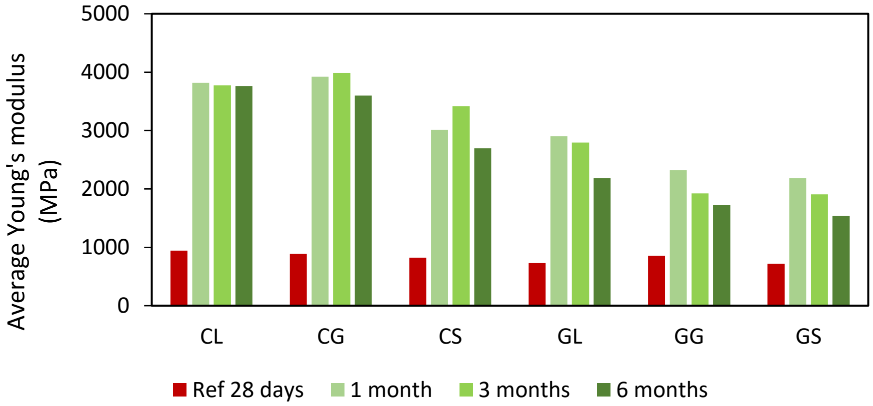

c)

Fig. 13. Overall average of mechanical properties of tested materials with submersion time: a) flexural strength, b) compressive strength, c) Young's modulus. Standard deviation is not represented as the values could differ a lot between regions . For one regions , it was small, like in Fig. 12.

Contrary to what is commonly accepted, the flexural strength may decrease as well as the elastic modulus, against the behaviour in compression, as seen here. This case has already been documented in [30] on geopolymers in seawater and can be encountered depending on the material characteristics (density, homogeneity, etc.). The same phenomenon might happen for cement in seawater. However, a low Young's modulus can be beneficial to slow down the propagation of cracks [30]. In addition, this behaviour was not strictly characteristic of all samples for one given region taken individually. Gererally the medium-term durability of all formulations was demonstrated here, with an advantage for CX. The biocolonisation might also have been an asset to protect the materials as it can be the case for other applications [32] [33].

4. Conclusion

The aim of this work was to assess the behaviour of 3D printable mortar formulations towards marine fauna and flora and their durability in seawater at medium term (1, 3 and 6 months). Both are major parameters to consider when designing artificial reefs. Yet further analysis should be undertaken and reported for the longer term deployments.

Mortar formulations with limited environmental impact composed of either geopolymer or cement CEM III as binders and three kinds of sand were studied. Results showed that:

- Initial biocolonisation was better with CEM III compared to geopolymer-based formulations. However, both tend to reach the maximum colonisation rate.
- On average, mechanical properties were better with CEM III-based formulations over time.
- The trend was similar across regions.

Regarding biocolonisation and mechanical properties, initial results indicate that CEM III-based formulations should thus be prioritised over geopolymer-based formulations for the 3D-printing of full-scale artificial reefs. To date, the 12 and 24 months samples are still immersed and the monitoring of their biocolonisation and durability continues.

Acknowledgments

The results presented in this article were obtained in the framework of the collaborative project *Artificial Reef 3D Printing for Atlantic Area* (3DPARE), co-funded by the European Regional Development Fund through the European cross-border programme INTERREG Atlantic Area.

References

[1] Hess RW, Rushworth D, Hynes MV, Peters JE. Disposal options for ships (No. RAND/MR-1377-NAVY). RAND Corp Santa Monica CA; 2001.

[2] Crain CM, Halpern BS, Beck MW, Kappel CV. Understanding and managing human threats to the coastal marine environment. The Year in Ecology and Conservation Biology 2009;1162:39-62.

[3] Baine M. Artificial reefs: a review of their design, application, management and performance. Ocean Coastal Manage 2001;44:241-259.

[4] Firth LB, Knights AM, Bridger D, Evans AJ, Mieszkowska N, Moore PJ, O'Connor NE, Sheehan EV, Thompson RC, Hawkins SJ. Ocean Sprawl: Challenges and opportunities for biodiversity management in a changing world. Oceanography and Marine Biology 2016;54:193-269.

[5] Ino T. Historical review of artificial reef activities in Japan. In L Colunga and RB Stone (eds.), Proceedings of an international conference on artificial reefs 1974;21-23.

[6] Stone RB. A brief history of artificial reef activities in the United States. In L Colunga and RB Stone (eds.), Proceedings of an international conference on artificial reefs 1974;24-27.

[7] Thierry JM. Artificial reefs in Japan – A general outline. Aquacult Eng 1988;7:321-348.

[8] Lefevre JR, Duval C, Ragazzi M, Duclerc J. Récifs artificiels : analyse bibliographique; 1984.

[9] Barnabé G, Charbonnel E, Marinaro JY, Ody D, Francour P. Artificial reefs in France: analysis, assessments and prospects. In AC Jensen et al. (eds.), Artificial Reefs in European Seas 2000;167-184.

[10] Fabi G, Spagnolo A, Bellan-Santini D, Charbonnel E, Çiçek BA, Goutayer García JJ, Jensen AC, Kallianiotis A, Neves dos Santos M. Overview on artificial reefs in Europe. Braz J Oceanogr 2011;59(1):155-166.

[11] Jensen A. Artificial reefs of Europe: perspective and future. ICES J Mar Sci 2002;59:S3-S13.

[12] Bohnsack JA, Sutherland DL. Artificial reef research: a review with recommendations for future priorities. Bull Mar Sci 1985;37(1):11-39.

[13] Herbert RJH, Collins K, Mallinson J, Hall AE, Pegg J, Ross K, Clarke L, Clements T. Epibenthic and mobile species colonisation of a geotextile artificial surf reef on the south coast of England. PLOS One 2017;12:e0184100.

[14] Pickering H, Whitmarsh D. Artificial reefs and fisheries exploitation: a review of the 'attraction versus production' debate, the influence of design and its significance for policy. Fish Res 1997;31:39-59.

[15] Tessier A, Francour P, Charbonnel E, Dalias N, Bodilis P, Seaman W, Lenfant P. Assessment of French artificial reefs: due to limitations of research, trends may be misleading. Hydrobiologia 2015;753(1):1-29.

[16] Castège I, Milon E, Fourneau G, Tauzia A. First results of fauna community structure and dynamics on two artificial reefs in the south of the Bay of Biscay (France). Estuarine Coastal Shelf Sci 2016;179:172-180.

[17] Boskalis Magazine (2018). 3D Printed Reefs. 15 March 2018.

[18] Lukens RR, Selberg C (project coordinators). Guidelines for marine artificial reef materials. Second edition. A joint publication of the Gulf and Atlantic States Marine Fisheries Commission; 2004.

[19] Habert G, d'Espinose de Lacaillerie JB, Roussel N. An environmental evaluation of geopolymer based concrete production: reviewing current research trends. J Cleaner Prod 2011;19:1229-1238.

[20] Polder RB, Nijland TG, de Rooij MR. Slag cement concrete – The Dutch Experience: Etatsprogrammet Varige konstruksjoner 2012-2015; 2014.

[21] Marion GM, Millero FJ, Camões MF, Spitzer P, Feistel R, Chen CTA (2011). pH of seawater. Mar Chem 2011;126:89-96.

[22] Halevy I, Bachan A. The geologic history of seawater pH. Science 2017;355(6329):1069-1071

[23] Aly Z, Vance ER, Perera DS, Hanna JV, Griffith CS, Davis J, Durce D. Aqueous leachability of metakaolin-based geopolymers with molar ratios of Si/Al = 1.5—4. J Nucl Mater 2008;378(2):172-179.

[24] Wahl M. Marine epibiosis. I. Fouling and antifouling: some basic aspects. Mar Ecol Prog Ser 1989;58:175-189.

[25] Novais RM, Buruberri LH, Seabra MP, Bajare D, Labrincha JA. Novel porous fly ash-containing geopolymers for pH buffering applications. J Cleaner Prod 2016;124:395-404.

[26] Matsunaga H, Tanishiki K, Tsuzimoto K. Environment-friendly block, “Ferroform”, made from steel slag. JFE GIHO 2008;19:13-17.

[27] Dobretsov S, Abed RMM, Teplitski M. Mini-review: Inhibition of biofouling by marine microorganisms. Biofouling 2013;29(4):423-441.

[28] McManus RS, Archibald N, Comber S, Knights AM, Thompson RC, Firth LB. Partial replacement of cement for waste aggregates in concrete coastal and marine infrastructure: A foundation for ecological enhancement? Ecol Eng 2018;120:655-667.

[29] Gunasekara C, Law DW, Setunge S. Long term permeation properties of different fly ash geopolymer concretes. Constr Build Mater 2016;124:352-362.

[30] Olivia M. Durability related properties of low calcium flash ash based geopolymer concrete. PhD thesis. Curtin University, Perth, Australia; 2011.

[31] Van Rompaey G. Étude de la réactivité des ciments riches en laitier, à basse température et à temps court, sans ajout chloré. PhD thesis. Université Libre de Bruxelles, Brussels, Belgium; 2006.

[32] Shifler DA. Understanding material interactions in marine environments to promote extended structural life. Corros Sci 2005;47:2335-2352.

[33] Lv J, Mao J, Ba H. Influence of marine microorganisms on the permeability and microstructure of mortar. Constr Build Mater 2015;77:33-40.